Materials Research Bulletin 68 (2015) 80–86

Contents lists available at ScienceDirect

Materials Research Bulletin

journal homepage: www.elsevier.com/locate/matresbu

Low-cost spray-processed $Ag_{1-x}Cu_xInS_2$ nano-films: Structural and functional investigation within the Lattice Compatibility Theory framework

D. Gherouel [a], A. Yumak [b], M. Znaidi [c], A. Bouzidi [a], K. Boubaker [a,*], N. Yacoubi [c], M. Amlouk [a]

[a] Unité de Physique des Dispositifs à Semi-conducteurs, Faculté des Sciences de Tunis, Tunis El Manar University, 2092 Tunis, Tunisia
[b] Physics Department, The Faculty of Arts and Science,Marmara University, 34722 Göztepe, Istanbul, Turkey
[c] Institut Préparatoire Aux Etudes d'Ingénieurs de Nabeul, Merazka, 8000 Nabeul, Tunisia

ARTICLE INFO

Article history:
Received 2 August 2014
Received in revised form 13 March 2015
Accepted 17 March 2015
Available online 19 March 2015

Keywords:
A. Alloys
B. Vapor deposition
C. X-ray diffraction
B. Lattice dynamics

ABSTRACT

This work deals with some structural and optical investigations about $Cu_xAg_{1-x}InS_2$ alloys sprayed films and the beneficial effect of copper incorporation in $AgInS_2$ ternary matrices. The main purpose of this work is to obtain the band gap energy E_g as well as different lattice parameters. The studied properties led to reaching minimum of lattice mismatch between absorber and buffer layers within solar cell devices. As a principal and original finding, the lattice compatibility between both silver and copper indium disulfide structures has been proposed as a guide for understanding kinetics of these materials crystallization.

1. Introduction

I–III–VI_2 chalcopyrite ternaries like $MInS_2$ (M=Cu, Ag, etc.) belong to an attractive family of material of photovoltaic cells and optoelectronic devices because of their band gap energy which matches solar spectrum and hence their good performance when subjected to solar illumination. In spite of their relatively high cost, they have been widely adopted as absorbers and buffers within thin film solar cells [1–4]. In the present study, the spray pyrolysis technique [5–8], which has not been widely adopted for such compounds, has been applied as a low-cost alternative for yielding cheap materials for wide range energy conversion application purpose. Each ternary compound has been fabricated in our laboratory using the spray pyrolisis method under appropriate conditions [6–8]. This method offers the decisive advantage of yielding n or p type $Cu_xAg_{1-x}InSe_2$ compound depending on precursors concentration and feeding rate [9–14].

2. Results and discussion

For the as-grown films, the optical properties were obtained from the analysis of the experimental recorded transmission and reflectance spectral data over the wavelength range 300–1800 nm using unpolarized light by means of a spectrophotometer (Shimadzu UV 3100S) [15]. Structural investigations have studied by means of X-ray diffraction apparatus (Panalytical X Pert PROMPD, $\lambda = 1.54056$ Å).

XRD spectra show in addition to the principle peak (1 1 2) the presence of (2 0 4), (3 1 2) and (1 1 6) additional peaks corresponding to the tetragonal structure of $AgInS_2$ with the presence of minor intensity peaks corresponding to $AgInS_2$ orthorhombic phase (Fig. 1). These results have been obtained in other works [5–12].

In the same way, the XRD analysis corresponding to $Cu_xAg_{1-x}InS_2$ exhibit a noticeable shift of (1 1 2) principle peak. It moved from 2θ position (27.08°) assigned to $AgInS_2$ material to (28.09°) angle corresponding to $CuInS_2$ compound. This proves the incorporation of Cu in the $AgInS_2$ tetragonal matrix by taking the silver place.

To reinforce this Cu behavior, some lattice calculations were carried out. First, the texture coefficient $TC_{(hkl)}$ values have been calculated from X-ray data, using the following formula [5]:

* Corresponding author. Tel.: +216 71811418.
E-mail address: mmbb11112000@yahoo.fr (K. Boubaker).

http://dx.doi.org/10.1016/j.materresbull.2015.03.038
0025-5408/

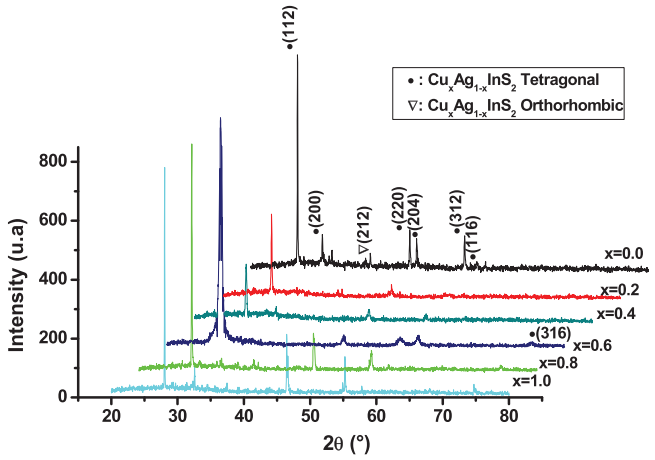

Fig. 1. XRD diagrams of $Cu_xAg_{1-x}InS_2$.

$$TC_{(hkl)} = \frac{I_{(hkl)}/I_{0(hkl)}}{N^{-1}\sum I_{(hkl)}/I_{0(hkl)}} \quad (1)$$

where $I_{(hkl)}$ is the measured relative intensity of (hkl) plane, $I_{0(hkl)}$ is the standard intensity of the same plane taken from the JCPDS card already mentioned, and N is the reflection number. $TC_{(hkl)}$ calculated values of the different sample are illustrated in Table 1.

For all the compounds, we note that the texture coefficient (TC) which indicates maximum preferred orientation (1 1 2). In addition, the interplanar spacing d_{112} values of these thin films were also calculated by using Bragg equation:

$$2d_{112}\sin\theta = n\lambda \quad (2)$$

Fig. 2 shows that the values of the distance d_{112} decreased with the increasing of the x ratio. This variation of the values of d_{112} of $Cu_xAg_{1-x}InS_2$ thin films with the x ratio obeys the empirical law:

$$y = A + B_1 \times x + B_2 \times x^2 \quad (3)$$

where A is the value of d_{112} of $Cu_xAg_{1-x}InS_2$ for the ratio $x = 0$, B_1 and B_2 are the fitted values found for these quaternaries (Table 2).

On the other hand, the average crystallite size D values are obtained (Fig. 3) from the Scherrer formula:

$$D = \frac{K\lambda}{\beta\cos\theta} \quad (4)$$

where k is constant $k = 0.9$. λ the length of wave $\lambda = 1.5418$ Å. β is the full width at half maximum and θ is the angle of strong peak.

The crystallite size obeys also to the same law ($y = A + B_1 \times x + B_2 \times x^2$) with A,B_1 and B_2 are constant. Their fitted values are listed in Table 2. This phenomenon of decreasing in the crystallite size ($D < 100$ nm) for films having $0.2 \le x \le 4$ can be explained by the poverty crystallization which is affected by the penetration of copper in the structure of $AgInS_2$ compound to form the quaternaries $Cu_xAg_{1-x}InS_2$. This result was shown in the other works [16]. When x is equal to unity, the $CuInS_2$ was formed and its crystallization is improved ($D = 196.95$ nm).

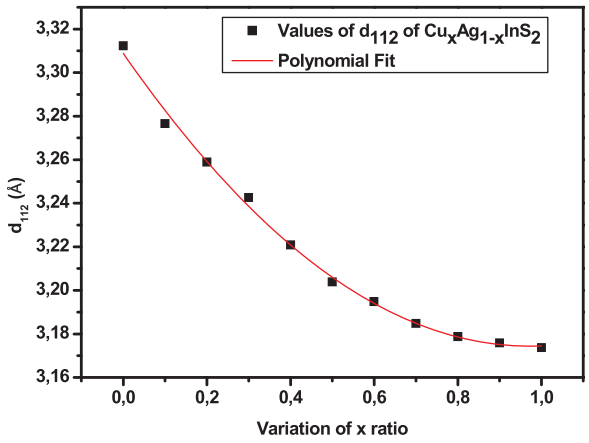

Fig. 2. The variation of d_{112} (Å) of $Cu_xAg_{1-x}InS_2$ with the x ratio.

In the same way, the microstrain (ξ) was calculated (Fig. 4) by the formula below [5]:

Table 2
Values of lattice constant of structural parameters of $Cu_xAg_{1-x}InS_2$.

	A	B_1	B_2
d_{112} (Å)	1.70	−0.13	0.06
D (nm)	155.66	−184.71	246.86
Microstrain	9.30E-4	1.53E-3	−2.17E-3

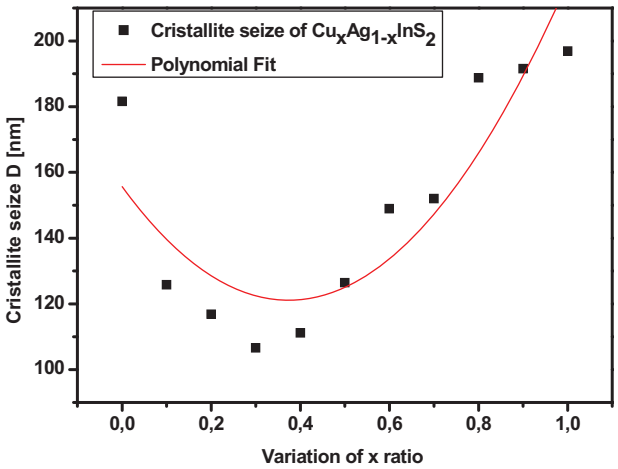

Fig. 3. The variation of the crystallite size D (nm) of $Cu_xAg_{1-x}InS_2$ with the x ratio.

Table 1
Values of texture coefficients of $Cu_xAg_{1-x}InS_2$ alloys.

	$Cu_xAg_{1-x}InS_2$ sprayed thin films										
	$x=0$	$x=0.1$	$x=0.2$	$x=0.3$	$x=0.4$	$x=0.5$	$x=0.6$	$x=0.7$	$x=0.8$	$x=0.9$	$x=1$
$TC_{(112)}$	0.29	0.37	0.35	0.32	0.36	0.23	0.33	0.25	0.27	0.26	0.45
$TC_{(200)}$	0.24	0.29	0.24	0.25	0.27	0.16	0.093	0.22	0.19	0.19	0.10
$TC_{(220)}$	0.20	0.30	0.12	0	0	0	0	0	0	0	0
$TC_{(204)}$	0.10	0.11	0.08	0.15	0.17	0.20	0.17	0.13	0.17	0.16	0.05
$TC_{(312)}$	0.13	0.10	0.19	0.11	0	0	0	0	0	0	0
$TC_{(116)}$	0.09	0	0	0.15	0.21	0.17	0.25	0.22	0.21	0.19	0.19
$TC_{(316)}$	0	0	0	0	0	0.08	0.12	0.09	0.10	0.08	0.14